

Modelling the emission of nitrogen-bearing molecules towards the solar type protostar IRAS16293-2422

A. Hernández-Gómez^{1,2}, E. Caux², L. Loinard¹ and S. Bottinelli²

¹Instituto de Radioastronomía y Astrofísica, Universidad Nacional Autónoma de México, Morelia 58089, Mexico

²IRAP, Université de Toulouse, CNRS, UPS, CNES, Toulouse, France

Abstract. Nitrogen, one of the most abundant elements in the Universe is a fundamental element of molecules which are crucial for life. We present here the modelling of the emission of two of the simplest nitrogen-bearing molecules, CN and NO, with a non-LTE radiative transfer code in IRAS16293-2422, a class 0 low-mass protostar. In this model, we assumed IRAS16293-2422 is formed by 2 compact, hot and dense sources embedded in a three layers of envelope.

Keywords. Protostars, molecular emission, non-LTE modelling.

1. Introduction

Nitrogen is one of the most abundant elements in the Universe. Nitrogen-bearing molecules are found in several astrophysical environments such as star-forming regions, protoplanetary disks, pre-stellar cores, comets, etc. In particular, a considerable amount of molecules associated with life contain nitrogen in their structure. For this reason, it is of vital importance to understand the formation and evolution of such molecules in early stages of star formation. The protostar IRAS16293-2422 is a very well known protostar located in the rho Ophiuchus star-forming region at 120 pc and has been identified as a binary system from interferometric observations. Large molecular surveys toward this source have revealed thousands of line transitions from tens of molecular species towards both binary components and the large envelope surrounding them (including many nitrogen-bearing species). Its proximity and its chemical wealth makes IRAS16293-2422 the ideal laboratory to probe not only the chemistry, but also the clustered star formation in detail. Two of the simplest nitrogen-bearing molecules are CN and NO. These molecules are crucial in the chemical network for the formation of molecular nitrogen, and other important molecules such as HCN, HNC, N₂H⁺, NH₃, etc. We present here the modelling of the emission of CN and NO with a non-LTE radiative transfer code considering that IRAS16293-2422 is formed by 2 compact, hot and dense sources and has three layers composing the envelope.

2. The physical model of IRAS16293-2422

To model the line emission of both CN and NO, we need information about the line profiles of different transitions over a wide range of excitation energies. For that, we have used data from the TIMASSS molecular survey (Caux *et al.* 2011) carried out toward this source (covering a frequency range between 80 – 500 GHz) using the IRAM, APEX and JCMT single-dish radiotelescopes, and the CHESSE survey (Ceccarelli *et al.* 2010) (in the 0.5 – 1 THz frequency range) with the HIFI instrument onboard the ESA Herschel Space

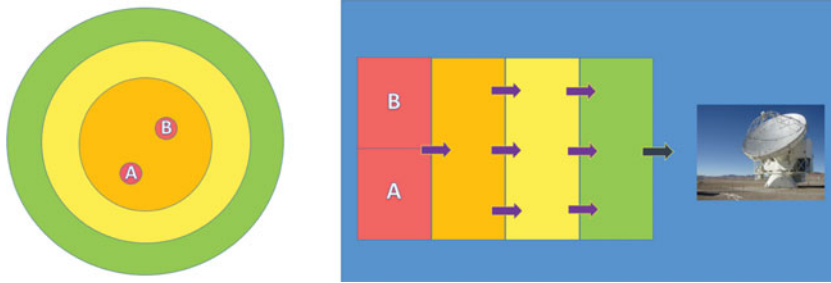


Figure 1. **Left.** Illustration of the physical structure of IRAS16293 used for the radiative transfer modelling. Both components of the binary system A and B are shown, along with the three components associated with the inner and external parts of the envelope of the protostar. **Right.** Model of the five physical components as slabs used for the CASSIS-RADEX modelling. The inner sources A and B (red) are within the same slab and are not interacting with each other. The output spectra of these two components thus interact with the internal warm layer of the envelope (orange), and the resulting spectrum subsequently interacts with the external cold layers of the envelope (yellow and green). The purple arrows indicates that the emission is calculated along all the slabs, while the black arrow indicates the final computed emission though all the slabs which is then diluted in the corresponding telescope beam.

Observatory. We assumed that the emission originates from five physical components as described in Figure 1.

3. Cyanide (CN) and nitric monoxide (NO) emission

In order to model the CN and NO emission, we have used the non-LTE code RADEX (van der Tak *et al.* 2007) inside CASSIS[†], performing a Monte Carlo Markov Chain Method minimisation to compute the best-fit spectra. Each physical component is constrained by 6 physical properties, the column density N , the kinetic temperature T_{kin} , the linewidth FWHM, the source size, the source V_{LSR} and the H_2 density, for a total of 30 free parameters. For CN, we have fixed the size and the H_2 density for all the components and the T_{kin} of the 2 hot cores from data in the literature. The size of the cold layers has been set to $100''$ to ensure they fill the telescope beams. For NO, we have first used the same free parameters, but as we found physical properties very close to the CN ones, we finally fixed them for all components to the values obtained for the CN best-fit. Results are summarized in Table 1, Figure 2 and Figure 3.

4. Discussion

Some of the CN physical properties (V_{LSR} , FWHM) are strongly constrained by the very high resolution spectra of the CN (3–2) lines observed with APEX around 340 GHz (see Figure 2). But some others are either degenerated (size, $N(\text{CN})$), or not well constrained (T_{kin}) because of the lack of spectral resolution for the CN (2–1) and (1–0) lines, that can bias the model. Additional observations at high resolution have been requested for both series of lines. With these data in hands, we will try to model simultaneously all N-bearing species observed either in the cold layers (NH, NH_2) or in the warm envelope (HCN, HNC, HC_3N , HC_5N , CH_3CN , N_2H^+) of IRAS16293, or in both (CN, NO, NH_3 , HNC, see poster from Hernández-Gómez, this conference). If detected we will also use the isotopes (^{13}C and ^{15}N) and deuterated counterparts (for NH, NH_2 , NH_3 , HCN, HNC,

[†] <http://cassis.irap.omp.eu>

Component	N(CN) (cm^{-2})	T_{kin} (K)	FWHM (km s^{-1})	V_{LSR} (km s^{-1})	Size ($''$)	$n(\text{H}_2)$ (cm^{-3})
IRAS16293A	$(2.2 \pm 0.45) \times 10^{14}$	100.0	2.2 ± 0.05	6.0	2.0	1.0×10^8
IRAS16293B	$(9.7 \pm 0.2) \times 10^{14}$	100.0	0.62 ± 0.05	3.2	1.0	1.0×10^8
Warm envelope	$(4.5 \pm 0.27) \times 10^{13}$	25.0 ± 1.0	2.13 ± 0.06	3.9 ± 0.04	17.3 ± 0.6	1.0×10^7
Cold layer 1	$(2.0 \pm 0.2) \times 10^{14}$	12.5 ± 0.7	0.27 ± 0.01	4.0 ± 0.01	100.0	3.0×10^4
Cold layer 2	$(1.2 \pm 0.16) \times 10^{14}$	16.5 ± 0.5	0.62 ± 0.01	4.1 ± 0.02	100.0	3.0×10^4

Component	N(NO) (cm^{-2})	T_{kin} (K)	FWHM (km s^{-1})	V_{LSR} (km s^{-1})	Size ($''$)	$n(\text{H}_2)$ (cm^{-3})
IRAS16293A	$(1.6 \pm 0.25) \times 10^{16}$	100.0	2.2	6.0	2.0	1.0×10^8
IRAS16293B	$(2.4 \pm 0.25) \times 10^{16}$	100.0	0.62	3.2	1.0	1.0×10^8
Warm envelope	$(1.0 \pm 0.1) \times 10^{15}$	25.0	2.13	3.9	17.3	1.0×10^7
Cold layer 1	$(8.8 \pm 4.3) \times 10^{13}$	12.5	0.27	4.0	100.0	3.0×10^4
Cold layer 2	$(6.1 \pm 2.4) \times 10^{13}$	16.5	0.62	4.1	100.0	3.0×10^4

Table 1. Assumed physical parameters and best fitted ones using the CASSIS-RADEX MCMC minimisation for all 5 components. CN (top) and NO (bottom).

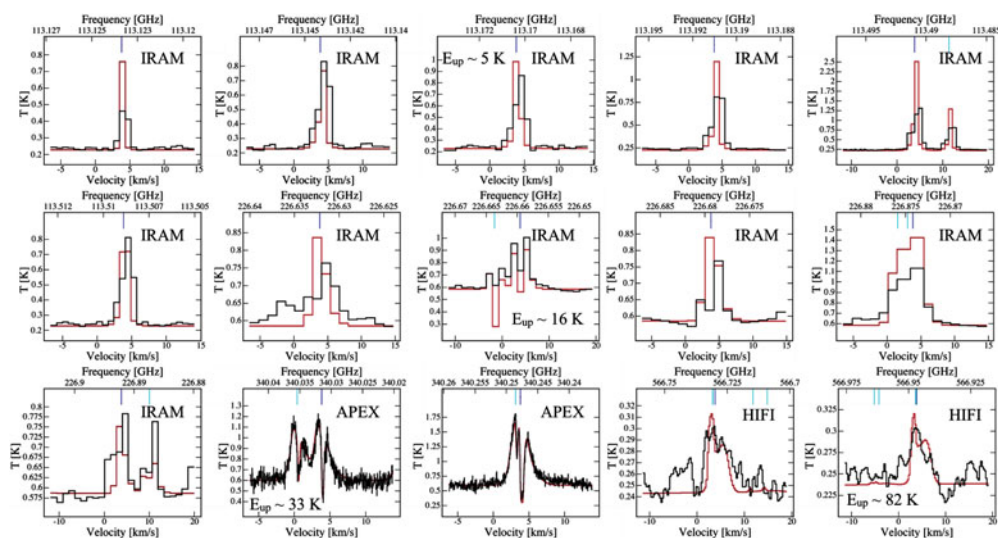


Figure 2. Observed (black) and predicted (red) CN lines modelled with CASSIS-RADEX. CN line frequencies are from CDMS (Müller *et al.* 2001). IRAM : CN (1–0) & (2–1). APEX : CN (3–2). Herschel-HIFI : CN (5–4). We used the collisional coefficients with He scaled by 1.37 as though they are for H_2 from Lique *et al.* (2009).

HC_3N , CH_3CN and HNCO). Interferometric data (SMA, ALMA) will help to constrain the physical properties of the 2 hot corinos, I16293A and I16293B. Finally, we will run the Nautilus chemical code (Ruaud *et al.* 2016) and the LIME 3D radiative transfer code (Brinch & Hogerheijde, 2010) using GASS (Quénard *et al.* 2017) to fully constrain the chemical and physical properties of the 5 identified components.

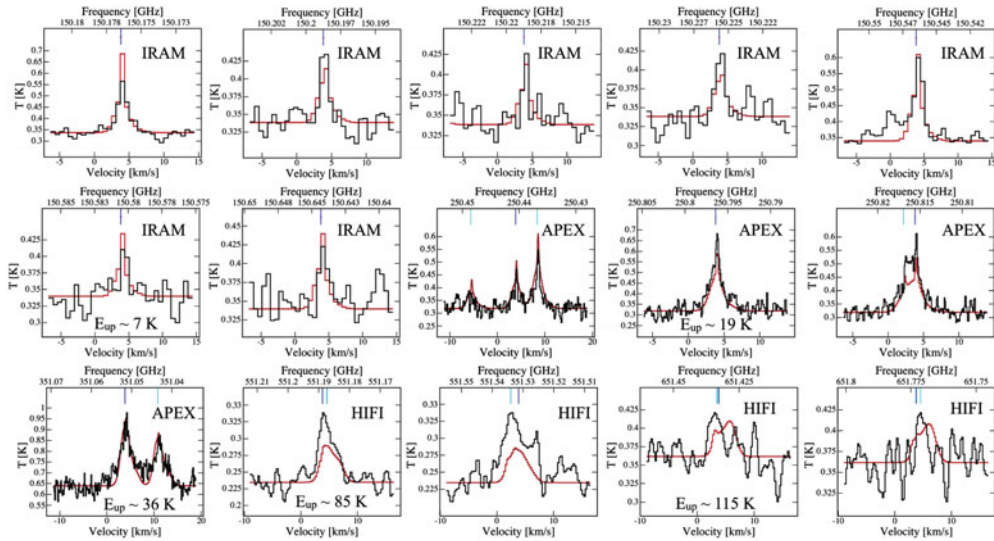


Figure 3. Observed (black) and predicted (red) NO lines modelled with CASSIS-RADEX. NO line frequencies are from CDMS. IRAM : NO (2–1). APEX : NO (3–2) & (4–3). Herschel-HIFI : NO (6–5) & (6–6). We used the collisional coefficients with He scaled by 1.37 as though they are for H₂ from Lique *et al.* (2009).

References

- Brinch, C. & Hogerheijde, M. R. 2010, *A&A*, 523, A25
 Caux, E., Kahane, C., Castets, A., *et al.* 2011, *A&A*, 532, A23
 Ceccarelli, C., Bacmann, A., Boogert, A., *et al.* 2010, *A&A*, 521, L22
 Lique, F., van der Tak, F. F. S., Klos, J., Bulthuis, J., & Alexander, M. H. 2009, *A&A*, 493, 557
 Lique *et al.* 2010, *J. Chem. Phys.*, 132, 024303
 Müller, H. S. P., Thorwirth, S., Roth, D. A., & Winnewisser, G. 2001, *A&A*, 370, L49
 Quénard, D., Bottinelli, S., & Caux, E., 2017, *MNRAS*, 468, 685
 Ruaud, M., Wakelam, V., & Hersant, F., 2016, *MNRAS*, 459, 3756
 van der Tak, F. F. S., Black, J. H., Schöier, F. L., Jansen, D. J., & van Dishoeck, E. F., 2007, *A&A*, 468, 627